arXiv preprint

Orientation selectivity analysis for integrated affine quasi quadrature models of complex cells

Tony Lindeberg

Abstract This paper presents an analysis of the orientation selectivity properties of idealized models of complex cells in terms of affine quasi quadrature measures, which combine the responses of idealized models of simple cells in terms of affine Gaussian derivatives by (i) pointwise squaring, (ii) summation of responses for different orders of spatial derivation and (iii) spatial integration. Specifically, this paper explores the consequences of assuming that the family of spatial receptive fields should be covariant under spatial affine transformations, thereby implying that the receptive fields ought to span a variability over the degree of elongation. We investigate the theoretical properties of three main ways of defining idealized models of complex cells and compare the predictions from these models to neurophysiologically obtained receptive field histograms over the resultant of biological orientation selectivity curves. It is shown that the extended modelling mechanisms lead to more uniform behaviour and a wider span over the values of the resultat that are covered, compared to earlier presented idealized models of complex cells without spatial integration. More generally, we propose that the presented methodology could be used as a new tool to evaluate other computational models of complex cells in relation to biological measurements.

Keywords Receptive field · Complex cell · Orientation selectivity · Elongation · Affine covariance · Vision

1 Introduction

To understand the functional properties of the visual system, it is essential to aim at bridging the gap between computational models on one side and neurophysiological measurements on the other side. Specifically, whenever possible, it is desirable to construct theoretically principled models, which could then lead to a deeper understanding of visual processing modules and also generate predictions for further biological experiments. One area where it indeed seems to be possible to bridge the gap between neurophysiological recordings and principled theory concerns the normative theory for visual receptive fields (Lindeberg 2021). This theory has been developed from principled assumptions regarding symmetry properties of an idealized vision system, and leads to a canonical family of linear receptive fields in terms of spatial derivatives of affine Gaussian kernels. Interestingly, the shapes of these idealized receptive fields do rather well correspond to the qualitative shapes of simple cells recorded by DeAngelis *et al.* (1995, 2004), Conway and Livingstone (2006) and Johnson *et al.* (2008).

One of the components in this normative theory for visual receptive fields is the assumption that the family of receptive fields ought to be covariant under spatial affine transformations, so as to enable more robust processing of the image data as variations in the viewing conditions imply variabilities in the image data caused by natural image transformations. Specifically, if an observer views the same object from different distances and viewing directions, the local image patterns will be deformed by the varying parameters of the perspective transformations, which to first order can be approximated by local affine transformations. In the area of computer vision, it has specifically been shown that the property of covariance under spatial affine transformations, referred to as affine covariance, enables more accurate estimation of surface orientation, compared to using only isotropic receptive fields that do not support affine covariance (Lindeberg and Gårding 1997).

To implement affine covariance in a vision system corresponds to using receptive field shapes subject to different affine spatial transformations, and will thereby specifi-

The support from the Swedish Research Council (contract 2022-02969) is gratefully acknowledged.

Computational Brain Science Lab, Division of Computational Science and Technology, KTH Royal Institute of Technology, SE-100 44 Stockholm, Sweden. E-mail: tony@kth.se. ORCID: 0000-0002-9081-2170.

cally imply that receptive fields ought to be present for different degrees of elongation. In a companion work (Lindeberg 2024a), we have indeed investigated the consistency of that affine covariant hypothesis with neurophysiological measurements of the resultant of orientation selectivity curves obtained by Goris *et al.* (2015). There, we showed that predictions generated from idealized models of simple cells in terms of Gaussian derivatives are for idealized model of simple cells in reasonable agreement with biological orientation selectivity histograms, and thereby consistent with an expansion of the receptive field shapes over the degree of elongation in the primary visual cortex of higher mammals.

The modelling of complex cells performed in (Lindeberg 2024a) was, however, based on very much simplified models in terms of *pointwise* non-linear combinations of responses of simple cells, and thus not involving any spatial integration of the non-linear combinations over extended regions in the image domain. Additionally, the modelling of complex cells in (Lindeberg 2024a) was based on input from simple cells up to only order two, and not involving simple cells up to order 4, which were shown to lead to better agreement between the predicted orientation selectivity histograms and the actual biological orientation selectivity histograms accumulated by Goris *et al.* (2015). The subject of this paper is to investigate a set of extended models of complex cells, and to demonstrate that these models offer a potential to lead to better agreement with biological orientation selectivity histograms compared to previous work.

In this way, we will thus specifically demonstrate that the resulting modelling of complex cells is also consistent with an expansion of the receptive field shapes over the degree of elongation, and in this way consistent with the wider hypothesis about affine covariant visual receptive fields, previously proposed in Lindeberg (2021, 2023).

2 Methods

2.1 Related work

Orientation selectivity properties of biological neurons have been studied by Watkins and Berkley (1974), Rose and Blakemore (1974), Schiller *et al.* (1976), Albright (1984), Ringach *et al.* (2002), Nauhaus *et al.* (2008), Scholl *et al.* (2013), Sadeh and Rotter (2014), Goris *et al.* (2015) and Sasaki *et al.* (2015). Biological mechanisms for achieving orientation selectivity have also been investigated by Somers *et al.* (1995), Sompolinsky and Shapley (1997), Carandini and Ringach (1997), Lampl *et al.* (2001), Ferster and Miller (2000), Shapley *et al.* (2003), Seriès *et al.* (2004), Hansel and van Vreeswijk (2012), Moldakarimov *et al.* (2014), Gonzalo Cogno and Mato (2015), Priebe (2016), Pattadkal *et al.* (2018), Nguyen and Freeman (2019), Merkt *et al.* (2019), Wei *et al.* (2022) and Wang *et al.* (2024). In this paper, our focus is, however, not on neural mechanisms, but on *functional properties* at a macroscopic level.

Receptive field models of simple in terms of Gaussian derivatives have been formulated by Koenderink and van Doorn (1984, 1987, 1992), Young and his co-workers (1987, 2001, 2001) and Lindeberg 2013, 2021), and in terms of Gabor functions by Marcelja (1980), Jones and Palmer (1987a, 1987b) and Porat and Zeevi (1988). More extensive theoretical models based on Gaussian derivatives have also been expressed by Lowe (2000), May and Georgeson (2007), Hesse and Georgeson (2005), Georgeson *et al.* (2007), Hansen and Neumann (2008), Wallis and Georgeson (2009), Wang and Spratling (2016), Pei *et al.* (2016), Ghodrati *et al.* (2017), Kristensen and Sandberg (2021), Abballe and Asari (2022), Ruslim *et al.* (2023) and Wendt and Faul (2024).

The taxonomy into simple and complex cells in the primary visual cortex was proposed in the pioneering work by Hubel and Wiesel (1959, 1962, 1968, 2005). More extensive analysis of properties of simple cells have then been presented by DeAngelis *et al.* (1995, 2004), Ringach (2002, 2004), Conway and Livingstone (2006), Johnson *et al.* (2008), Walker *et al.* (2019) and De and Horwitz (2021), and regarding complex cells by Movshon *et al.* (1978), Emerson *et al.* (1987), Martinez and Alonso (2001), Touryan *et al.* (2002, 2005), Rust *et al.* (2005), van Kleef *et al.* (2010), Goris *et al.* (2015), Li *et al.* (2015) and Almasi *et al.* (2020), as well as modelled computationally by Adelson and Bergen (1985), Heeger (1992), Serre and Riesenhuber (2004), Einhäuser *et al.* (2002), Kording *et al.* (2004), Merolla and Boahen (2004), Berkes and Wiscott (2005), Carandini (2006), Hansard and Horaud (2011), Franciosini *et al.* (2019), Lindeberg (2020), Lian *et al.* (2021), Oleskiw *et al.* (2024), Yedjour and Yedjour (2024) and Nguyen *et al.* (2024).

2.2 Background theory

In this section, we will describe basic properties of the idealized models for idealized models of receptive fields and their orientation selectivity properties, which we will then build upon and extend in Section 3.

2.2.1 Idealized models for spatial receptive fields

For modelling simple and complex cells in the primary visual cortex, we will build upon the generalized Gaussian derivative model for visual receptive fields proposed in Lindeberg (2013, 2021) and further developed in Lindeberg (2023, 2024c, 2025).

Models for simple cells. According to this theory, linear models of purely spatial receptive fields corresponding to simple

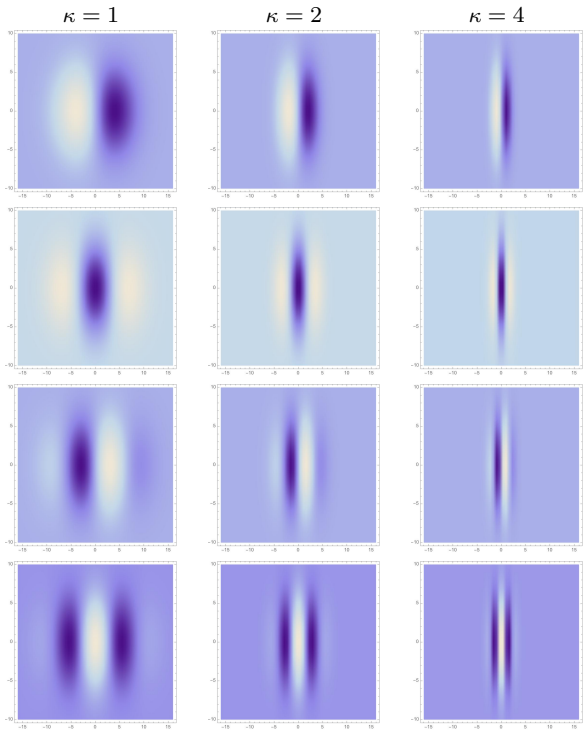

Fig. 1 Distribution of affine Gaussian derivative receptive fields (for the preferred image orientation $\varphi = 0$) over the scale parameter ratio $\kappa = \sigma_2/\sigma_1$ between 1 to 4, from left to right. Here, the vertical scale parameter kept is constant $\sigma_2 = 4$, while the horizontal scale parameter is smaller $\sigma_1 \leq \sigma_2$. (first row) First-order directional derivatives according to (1) for $m = 1$. (second row) Second-order directional derivatives according to (1) for $m = 2$. (third row) Third-order directional derivatives according to (1) for $m = 3$. (fourth row) Fourth-order directional derivatives according to (1) for $m = 4$. (Horizontal axes: image coordinate $x_1 \in [-16, 16]$. Vertical axes: image coordinate $x_2 \in [-16, 16]$.)

cells are formulated in terms of affine Gaussian derivatives of the form

$$T_{\text{simple}}(x_1, x_2;\ \sigma_\varphi, \varphi, \Sigma_\varphi, m) = T_{\varphi^m,\text{norm}}(x_1, x_2;\ \sigma_\varphi, \Sigma_\varphi) = \sigma_\varphi^m\, \partial_\varphi^m\, (g(x_1, x_2;\ \Sigma_\varphi)), \tag{1}$$

where

- $\varphi \in [-\pi, \pi]$ is the preferred orientation of the receptive field,
- $\sigma_\varphi \in \mathbb{R}_+$ is the amount of spatial smoothing,
- $\partial_\varphi^m = (\cos\varphi\, \partial_{x_1} + \sin\varphi\, \partial_{x_2})^m$ is an m:th-order directional derivative operator, in the direction φ,
- Σ_φ is a 2×2 symmetric positive definite covariance matrix, with one of its eigenvectors in the direction of φ,
- $g(x;\ \Sigma_\varphi)$ is a 2-D affine Gaussian kernel with its shape determined by the covariance matrix Σ_φ

$$g(x;\ \Sigma_\varphi) = \frac{1}{2\pi\sqrt{\det \Sigma_\varphi}} e^{-x^T \Sigma_\varphi^{-1} x/2} \tag{2}$$

for $x = (x_1, x_2)^T \in \mathbb{R}^2$.

In Lindeberg (2021), it was demonstrated that idealized receptive field models of this type do rather well model the qualitative shape of biological simple cells as obtained by neurophysiological measurements by DeAngelis *et al.* (1995, 2004), Conway and Livingstone (2006) and Johnson *et al.* (2008).

Figure 1 shows examples of such receptive fields for different orders of spatial differentiation $m \in \{1, 2, 3, 4\}$ and different values of the scale parameter ratio $\kappa = \sigma_2/\sigma_1 \in \{1, 2, 4\}$ between here the vertical and the horizontal scale parameters σ_2 and σ_1, respectively, for the here preferred orientation $\varphi = 0$ for the receptive fields. In addition to this illustrated variability over the degree of elongation, an idealized vision system should additionally comprise a variability over the preferred orientation φ of the receptive fields, and possibly also over the overall size of the receptive fields, as further developed in Lindeberg (2024b).

Models for complex cells. As a simplest possible extension to non-linear complex cells, an affine quasi-quadrature measure of the form (Lindeberg 2020 Equation (39))

$$\mathcal{Q}_{\varphi,12,\text{pt}} L = \sqrt{L_{\varphi,\text{norm}}^2 + C_\varphi\, L_{\varphi\varphi,\text{norm}}^2}, \tag{3}$$

was studied in Lindeberg (2024a), where

- $L_{\varphi,\text{norm}}$ and $L_{\varphi\varphi,\text{norm}}$ denote directional derivatives in the direction φ of orders 1 and 2 of convolutions of the input image $f(x_1, x_2)$ with affine Gaussian derivative kernels of the form (1):

$$L_{\varphi,\text{norm}}(x_1, x_2;\ \sigma_\varphi, \Sigma_\varphi) = = T_{\varphi,\text{norm}}(x_1, x_2;\ \sigma_\varphi, \Sigma_\varphi) * f(x_1, x_2), \tag{4}$$

$$L_{\varphi\varphi,\text{norm}}(x_1, x_2;\ \sigma_\varphi, \Sigma_\varphi) = = T_{\varphi\varphi,\text{norm}}(x_1, x_2;\ \sigma_\varphi, \Sigma_\varphi) * f(x_1, x_2), \tag{5}$$

- $C_\varphi > 0$ is a weighting factor between first and second-order information, which based on a theoretical analysis in (Lindeberg 2018) is often set to $C = 1/\sqrt{2}$.

This model is closely related to the energy model of complex cells proposed by Adelson and Bergen (1985) and Heeger (1992), as well as inspired by the fact that odd- and even-shaped receptive fields have been reported to occur in pairs (De Valois *et al.* 2000). The quasi quadrature serves as an approximation of a quadrature pair, as formulated based on a Hilbert transform (Bracewell 1999, pp. 267–272), although instead formulated in terms of affine Gaussian derivatives, which are then summed up in squares in to reduce the phase dependency, see Lindeberg (2020) for further details.

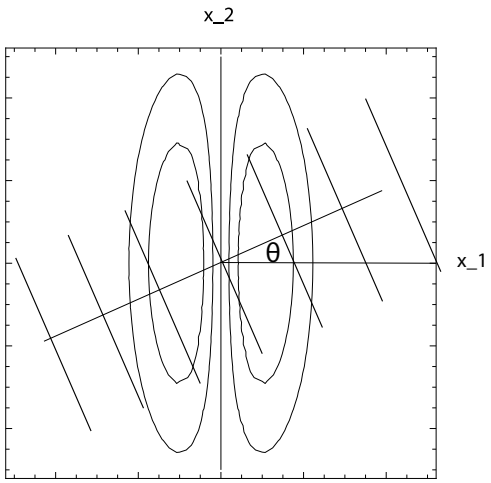

Fig. 2 To measure the orientation selectivity properties of an idealized receptive field (here illustrated by the level curves of a first-order derivative of an affine Gaussian kernel in the horizontal direction with preferred orientation $\varphi = 0$), we compute the response to a sine wave (here illustrated by a set of darker level lines corresponding to the spatial maxima and minima of the sine wave) with inclination angle θ. (Horizontal axis: spatial coordinate x_1. Vertical axis: spatial coordinate x_2.) (Illustration reproduced from Lindeberg (2025) OpenAccess.)

2.2.2 Orientation selectivity properties

In Lindeberg (2025, 2024a), the orientation selectivity properties of these idealized models of simple and complex cells were investigated in detail, by computing the responses to sine wave functions of the form

$$f(x_1, x_2) = \sin\left(\omega \cos(\theta)\, x_1 + \omega \sin(\theta)\, x_2 + \beta\right) \tag{6}$$

where $\theta \in [-\pi/2, \pi/2]$ denotes the inclination angle of the sine wave in relation to the preferred orientation $\varphi = 0$ of the receptive field and β denotes the phase, see Figure 2 for an illustration. Specifically, in Lindeberg (2025, 2024a), it was shown that with

$$\kappa = \frac{\sigma_2}{\sigma_1} \tag{7}$$

denoting the ratio between the scale parameters $\sigma_1 \in \mathbb{R}_+$ and $\sigma_2 \in \mathbb{R}_+$ of the affine Gaussian kernel in the preferred direction *vs.* the orthogonal direction of the receptive field, the orientation selectivity curves are of the form

$$r_\lambda(\theta) = \left(\frac{|\cos\theta|}{\sqrt{\cos^2\theta + \kappa^2 \sin^2\theta}} \right)^\lambda \tag{8}$$

with

- $\lambda = m$ for an m:th-order model of a simple cell of the form (1) for $m \in \{1, 2, 3, 4\}$ and
- $\lambda = 3/2$ for an idealized model of a complex cell of the form (3).

Notably, for all these idealized models of the receptive fields, a smaller value of the scale parameter ratio κ leads to wider orientation selectivity curves, whereas larger values of κ lead to more narrow orientation selectivity properties. In this respect, given the assumption that the affine Gaussian derivative model should constitute an appropriate model for the spatial component of simple cells, a variability in the degree of elongation of the receptive fields will correspond to a variability in the orientation selectivity and *vice versa*.

3 Results

3.1 Generalized idealized models of complex cells

In this work, we will extend the idealized model (3) for complex cells in two major ways:

- by adding a spatial integration stage, and
- considering derivatives up to order 4 in addition to derivatives up to order 2.

The motivation for adding a spatial integration stage is that the model for complex cell should then make use of input from more than two simple cells, specifically by accumulating input over multiple positions in the visual field.

The motivation for adding derivatives of higher order than 2 are: (i) to enable more narrow orientation selectivity properties and (ii) in Lindeberg (2024a) it was shown that models of simple cells up to order 4 lead to better agreement with the orientation selectivity histogram of simple cells recorded by Goris *et al.* (2015) than simple cells up to order 2.

Thus, if we let $L_{\varphi\varphi\varphi,\text{norm}}$ and $L_{\varphi\varphi\varphi\varphi,\text{norm}}$ denote the directional derivatives in the direction φ of orders 3 and 4 of convolutions of the input image $f(x_1, x_2)$ with affine Gaussian derivative kernels of the form (1):

$$L_{\varphi\varphi\varphi,\text{norm}}(x_1, x_2;\ \sigma_\varphi, \Sigma_\varphi) = \\ = T_{\varphi,\varphi\varphi,\text{norm}}(x_1, x_2;\ \sigma_\varphi, \Sigma_\varphi) * f(x_1, x_2), \tag{9}$$

$$L_{\varphi\varphi\varphi\varphi,\text{norm}}(x_1, x_2;\ \sigma_\varphi, \Sigma_\varphi) = \\ = T_{\varphi\varphi,\varphi\varphi,\text{norm}}(x_1, x_2;\ \sigma_\varphi, \Sigma_\varphi) * f(x_1, x_2), \tag{10}$$

as well as consider the previous definitions of $L_{\varphi,\text{norm}}$ and $L_{\varphi\varphi,\text{norm}}$ according to (4) and (5), we will consider the following new generalized and integrated affine quasi quadrature measures for modelling complex cells:

$$\mathcal{Q}_{\varphi,12,\text{int}} L = \\ = \sqrt{\sum_{m \in \{1,2\}} g(\cdot, \cdot;\ \gamma^2 \Sigma_\varphi) * C_\varphi^{m-1}\, L^2_{\varphi^m,\text{norm}}(\cdot, \cdot)} \tag{11}$$

$$\mathcal{Q}_{\varphi,1234,\text{int}} L = \\ = \sqrt{\sum_{m \in \{1,2,3,4\}} g(\cdot,\cdot;\ \gamma^2 \Sigma_\varphi) * C_\varphi^{m-1}\, L^2_{\varphi^m,\text{norm}}(\cdot,\cdot)} \tag{12}$$

$$\mathcal{Q}_{\varphi,34,\text{int}} L = \\ = \sqrt{\sum_{m \in \{3,4\}} g(\cdot,\cdot;\ \gamma^2 \Sigma_\varphi) * C_\varphi^{m-3}\, L^2_{\varphi^m,\text{norm}}(\cdot,\cdot)}, \tag{13}$$

where $g(\cdot,\cdot;\ \gamma^2 \Sigma_\varphi)$ for the relative integration scale $\gamma > 1$ denotes a spatially larger affine Gaussian kernel than the affine Gaussian kernel $g(\cdot,\cdot;\ \Sigma_\varphi)$ used for computing the receptive field responses $L_{\varphi^m,\text{norm}}$ for the idealized models of simple cells. In the following experiments to be reported, wewill throughout use the parameter setting $\gamma = 1/\sqrt{2}$.

Structurally, these expressions are similar in the sense that the squares of the directional derivative responses $L_{\varphi^m,\text{norm}}$ are first integrated for different orders m of spatial differentiation, and then summed of for different subsets $m \in \{1,2\}$, $m \in \{1,2,3,4\}$ and $m \in \{3,4\}$, respectively. Specifically, the first of these integrated affine quasi quadrature measures $\mathcal{Q}_{\varphi,12,\text{int}} L$ can basically be seen as a spatially integrated extension of the pointwise affine quasi quadrature measure $\mathcal{Q}_{\varphi,12,\text{pt}} L$ in (3).

3.2 Orientation selectivity curves for the generalized idealized models of complex cells

To characterize the orientation selectivity properties for the generalized integrated affine quasi quadrature measures (11), (12) and (13), let us first compute the responses $L_{\varphi^m,\text{norm}}$ for the underlying models of simple cells $T_{\varphi^m,\text{norm}}$ to a sine wave (6) according to Equations (29) and (35) in Lindeberg (2025)

$$L_{0,\text{norm}}(x_1, x_2;\ \sigma_1, \sigma_2) = \\ = \int_{\xi_1=-\infty}^{\infty} \int_{\xi_2=-\infty}^{\infty} T_{0,\text{norm}}(\xi_1, \xi_2;\ \sigma_1, \sigma_2) \\ \times f(x_1 - \xi_1, x_2 - \xi_2)\, d\xi_1 \xi_2 \\ = \omega\, \sigma_1 \cos(\theta)\, e^{-\frac{1}{2}\omega^2 (\sigma_1^2 \cos^2\theta + \sigma_2^2 \sin^2\theta)} \\ \times \cos(\omega \cos(\theta)\, x_1 + \omega \sin(\theta)\, x_2 + \beta), \tag{14}$$

$$L_{00,\text{norm}}(x_1, x_2;\ \sigma_1, \sigma_2) = \\ = \int_{\xi_1=-\infty}^{\infty} \int_{\xi_2=-\infty}^{\infty} T_{00,\text{norm}}(\xi_1, \xi_2;\ \sigma_1, \sigma_2) \\ \times f(x_1 - \xi_1, x_2 - \xi_2)\, d\xi_1 \xi_2 \\ = -\omega^2\, \sigma_1^2 \cos^2(\theta)\, e^{-\frac{1}{2}\omega^2 (\sigma_1^2 \cos^2\theta + \sigma_2^2 \sin^2\theta)} \\ \times \sin(\omega \cos(\theta)\, x_1 + \omega \sin(\theta)\, x_2 + \beta), \tag{15}$$

and according to Equations (36) and (42) in Lindeberg (2024a)

$$L_{000,\text{norm}}(x_1, x_2;\ \sigma_1, \sigma_2) = \\ = \int_{\xi_1=-\infty}^{\infty} \int_{\xi_2=-\infty}^{\infty} T_{000,\text{norm}}(\xi_1, \xi_2;\ \sigma_1, \sigma_2) \\ \times f(x_1 - \xi_1, x_2 - \xi_2)\, d\xi_1 \xi_2 \\ = -\omega^3\, \sigma_1^3 \cos^3(\theta)\, e^{-\frac{1}{2}\omega^2 (\sigma_1^2 \cos^2\theta + \sigma_2^2 \sin^2\theta)} \\ \times \cos(\omega \cos(\theta)\, x_1 + \omega \sin(\theta)\, x_2 + \beta), \tag{16}$$

$$L_{0000,\text{norm}}(x_1, x_2;\ \sigma_1, \sigma_2) = \\ = \int_{\xi_1=-\infty}^{\infty} \int_{\xi_2=-\infty}^{\infty} T_{0000,\text{norm}}(\xi_1, \xi_2;\ \sigma_1, \sigma_2) \\ \times f(x_1 - \xi_1, x_2 - \xi_2)\, d\xi_1 \xi_2 \\ = \omega^4\, \sigma_1^4 \cos^4(\theta)\, e^{-\frac{1}{2}\omega^2 (\sigma_1^2 \cos^2\theta + \sigma_2^2 \sin^2\theta)} \\ \times \sin(\omega \cos(\theta)\, x_1 + \omega \sin(\theta)\, x_2 + \beta), \tag{17}$$

where $\sigma_1 \in \mathbb{R}_+$ and $\sigma_2 \in \mathbb{R}_+$ denote the scale parameters of the affine Gaussian kernel in the horizontal and the vertical directions, respectively.

Let us next integrate the squares of these expressions spatially using a Gaussian window function with relative integration scale $\gamma > 1$, with the actual calculations performed in Mathematica, and leading to results that are unfortunately too complex to be reproduced here.

Let us furthermore for the parameterization of the vertical scale parameter $\sigma_2 = \kappa\, \sigma_1$ consider the angular frequencies $\hat{\omega}_1$, $\hat{\omega}_2$, $\hat{\omega}_3$ and $\hat{\omega}_4$ for which these expressions assume their maxima over angular frequencies according to Equations (33) and (38) in Lindeberg (2025)

$$\hat{\omega}_\varphi = \frac{1}{\sigma_1 \sqrt{\cos^2\theta + \kappa^2 \sin^2\theta}}, \tag{18}$$

$$\hat{\omega}_{\varphi\varphi} = \frac{\sqrt{2}}{\sigma_1 \sqrt{\cos^2\theta + \kappa^2 \sin^2\theta}}, \tag{19}$$

and according to Equations (40) and (45) in Lindeberg (2024a)

$$\hat{\omega}_{\varphi\varphi\varphi} = \frac{\sqrt{3}}{\sigma_1 \sqrt{\cos^2\theta + \kappa^2 \sin^2\theta}}, \tag{20}$$

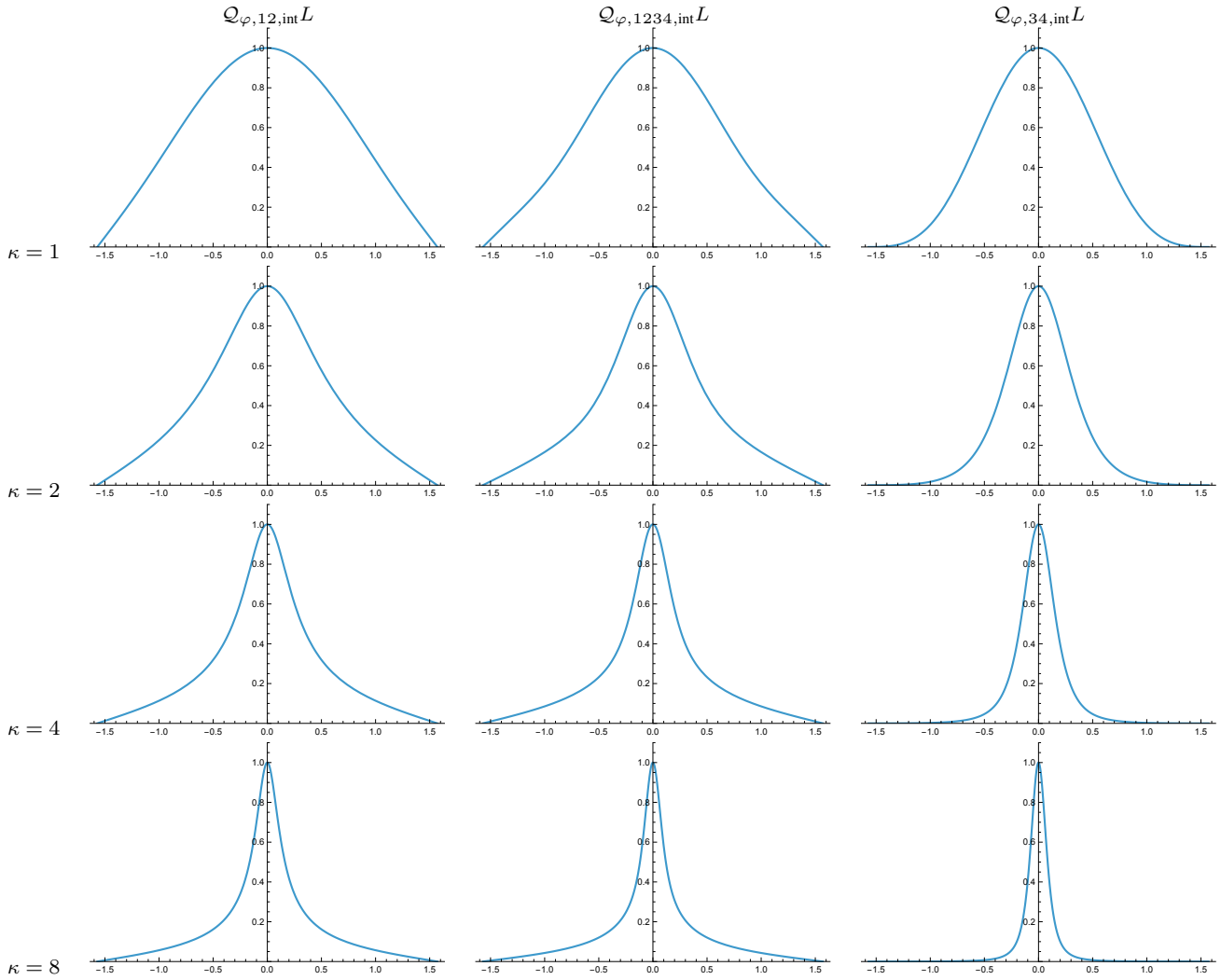

Fig. 3 Graphs of the orientation selectivity for the generalized integrated affine quasi quadrature measures $\mathcal{Q}_{\varphi,12,\mathrm{int}}L$ according to (11), $\mathcal{Q}_{\varphi,1234,\mathrm{int}}L$ according to (12) and $\mathcal{Q}_{\varphi,34,\mathrm{int}}L$ according to (13), which combine integrated squared values of affine Gaussian derivative responses for different combinations of orders of integration $m \in \{1, 2, 3, 4\}$ when applied to an ideal sine wave of the form (6) with the angular frequency of the sine wave adapted so as to evoke a maximally strong response over the angular frequencies according to (22), (23) and (24), respectively. The resulting orientation selectivity curves are shown for different values of the scale parameter ratio $\kappa = \sigma_2/\sigma_1$, which parameterizes the degree of elongation of the receptive fields. (top row) Results for $\kappa = 1$. (second row) Results for $\kappa = 2$. (third row) Results for $\kappa = 4$. (bottom row) Results for $\kappa = 8$. (Horizontal axes: orientation $\theta \in [-\pi/2, \pi/2]$. Vertical axes: Amplitude of the receptive field response relative to the maximum response obtained for $\theta = 0$.)

$$\hat{\omega}_{\varphi\varphi\varphi\varphi} = \frac{2}{\sigma_1 \sqrt{\cos^2\theta + \kappa^2 \sin^2\theta}}. \tag{21}$$

Given these preferred angular frequencies for the different orders of spatial integration, let us next for the composed integrated affine quasi quadrature measures (11), (12) and (13) choose the geometric averages of the respective components according to

$$\hat{\omega}_{12} = \sqrt{\hat{\omega}_{\varphi}\, \hat{\omega}_{\varphi\varphi}}, \tag{22}$$

$$\hat{\omega}_{1234} = \sqrt{\hat{\omega}_{\varphi}\, \hat{\omega}_{\varphi\varphi}\, \hat{\omega}_{\varphi\varphi\varphi}\, \hat{\omega}_{\varphi\varphi\varphi\varphi}}, \tag{23}$$

$$\hat{\omega}_{34} = \sqrt{\hat{\omega}_{\varphi\varphi}\, \hat{\omega}_{\varphi\varphi\varphi\varphi}}, \tag{24}$$

and adapt the angular frequency of the probing sine wave in these ways to the respective quasi quadrature measures $\mathcal{Q}_{\varphi,12,\mathrm{int}}L$ according to (11), $\mathcal{Q}_{\varphi,1234,\mathrm{int}}L$ according to (12) and $\mathcal{Q}_{\varphi,34,\mathrm{int}}L$ according to (13). This adaptation of the angular frequency of the sine wave to the internal parameters of the model of the complex cell corresponds to probing the corresponding complex cells for different values of the angular frequency ω and then choosing the orientation se-

lectivity curve for the angular frequency $\hat{\omega}$ that leads to the maximum response over all the frequencies ω.

Figure 3 shows the resulting orientation selectivity curves that we then obtain for different values of the scale parameter ratio κ, when using the relative integration scale $\gamma = 1/\sqrt{2}$ for the spatial integration stage and the weighting factor $C = 1/\sqrt{2}$ when combining the responses for different orders m of differentiation. As can be seen from these graphs, for all the three generalized integrated affine quasi quadrature measures, the orientation selectivity curves become sharper with increasing values of the scale parameter ratio κ. In this respect, these results are consistent with the previously reported results in Lindeberg (2025, 2024a).

Specifically, in relation to the previously recorded orientation selectivity curves for biological neurons reported in Nauhaus *et al.* (2008), and which span a variability in orientation selectivity from wide to narrow orientation selectivity properties, these results are consistent with what would be the case if the receptive fields in the primary visual cortex would span a variability in the degree of elongation, as proposed as a working hypothesis in Lindeberg (2023) Section 3.2.1 and further investigated in Lindeberg (2024a).

3.3 Orientation selectivity histograms for the generalized idealized models of complex cells

The previous analysis is *qualitative* in the sense that it shows that the orientation selectivity curves become sharper for increasing values of the scale parameter ratio κ, and also in the respect that a variability in the orientation selectivity properties is consistent with an underlying variability in the degree of elongation of the receptive fields.

To aim at a more *quantitative* analys, let us compare the result of our idealized integrated models of complex cells with the quantitative measurements of orientation selectivity histograms reported by Goris *et al.* (2015). They accumulated histograms of the absolute value of the resultant $|R|$ with the underlying complex-valued resultant of an orientation selectivity curve $r(\theta)$ of the form

$$R = \frac{\int_{\theta=-\pi}^{\pi} r(\theta)\, e^{2i\theta} d\theta}{\int_{\theta=-\pi}^{\pi} r(\theta)\, d\theta}. \tag{25}$$

The left figure in the top row in Figure 4 gives a schematic illustration of the results that they obtained, reflecting a significant variability in wide *vs.* narrow orientation selectivity properties for different biological complex cells. The right figure in the top row in Figure 4 shows a corresponding prediction of a histogram of the resultant of the orientation selectivity curves obtained in Lindeberg (2024a), based on the pointwise quasi quadrature measure $\mathcal{Q}_{\varphi,12,\text{pt}}L$ in (3), based on assuming that the scale parameter ratio κ would be uniformly distributed on a logarithmic scale over the interval $[1/\kappa_{\max}, \kappa_{max}]$ for the arbitrary choice of $\kappa_{max} = 8$.

As can be seen from the comparison between the biological results and the idealized modelling results, the distributions over the resultant $|R|$ is somewhat biased toward both smaller and larger values of $|R|$, compared to the neurophysiologically accumulated resultant histograms. A natural question to ask is hence if this behaviour would be different if using more developed models of complex cells, that also comprise a spatial integration stage and derivatives of higher order than 2.

The second row in Figure 4 show the result of computing the resultant measure $|R|$ as a function of the scale parameter ratio $\kappa = \sigma_2/\sigma_1$ for each one of the integrated affine quasi quadrature measures $\mathcal{Q}_{\varphi,12,\text{int}}L$, $\mathcal{Q}_{\varphi,1234,\text{int}}L$ and $\mathcal{Q}_{\varphi,34,\text{int}}L$ according to (11), (12) and (13).

The third row in Figure 4 show corresponding resultant histograms for each of these integrated affine quasi quadrature measures, when assuming a uniform distribution over a logarithmic parameterization of the scale parameter ratio κ over the interval $[1/\kappa_{\max}, \kappa_{\max}]$ for the again arbitrary value of $\kappa_{\max} = 8$. Such a logarithmic distribution constitutes a natural default prior for a strictly positive variable according to the (Jaynes 1968). The bottom row in Figure 4 shows a combined histogram of the integrated affine quasi quadrature measures $\mathcal{Q}_{\varphi,12,\text{int}}L$ and $\mathcal{Q}_{\varphi,34,\text{int}}L$, when assuming an equal number of idealized complex cells for these two types.

As can be seen from these histograms, the use of the integrated affine quasi quadrature measures $\mathcal{Q}_{\varphi,12,\text{int}}L$, $\mathcal{Q}_{\varphi,1234,\text{int}}L$ and $\mathcal{Q}_{\varphi,34,\text{int}}L$ leads to resultant histograms with different shapes than for pointwise quasi quadrature measure $\mathcal{Q}_{\varphi,12,\text{pt}}L$ previously studied in Lindeberg (2024a). Specifically, except for the peak at the bin corresponding to $|R| \in [0.6, 0.7]$, the resultant histogram of $\mathcal{Q}_{\varphi,1234,\text{int}}L$ is more uniform and without any bias the bias towards either smaller values of the resultant $|R|$ towards the bins $|R| \in [0.1, 0.2]$ and $|R| \in [0.7, 0.8]$ as for the resultant histogram of the pointwise quasi quadrature measure $\mathcal{Q}_{\varphi,12,\text{pt}}L$.

Additionally, when including third- and fourth-order terms, the integrated affine quasi quadrature measures $\mathcal{Q}_{\varphi,1234,\text{int}}L$ and $\mathcal{Q}_{\varphi,34,\text{int}}L$ lead to accumulations to the bins $|R| \in [0.8, 0.9]$ and $|R| \in [0.9, 1.0]$, while those bins are not really reached by the pointwise quasi quadrature measure $\mathcal{Q}_{\varphi,12,\text{pt}}L$. In these respects, this analysis suggests that the mechanisms of spatial integration and inclusion of higher-order terms than mere first- and second-order terms may be important to more quantitatively model the orientation selectivity properties of complex cells. Furthermore, one may speculate if a suitable reformulation of the non-linearities in the composed integrated affine quasi quadrature measures $\mathcal{Q}_{\varphi,1234,\text{int}}L$ could move the peak for the bin $|R| \in [0.6, 0.7]$ to the bin positions $|R| \in [0.3, 0.4]$ and $|R| \in [0.5, 0.6]$ that lead to peaks in the resultant histogram for the biological complex cells.

Based on these results, we therefore propose to include third- and fourth-order models of simple cells in addition

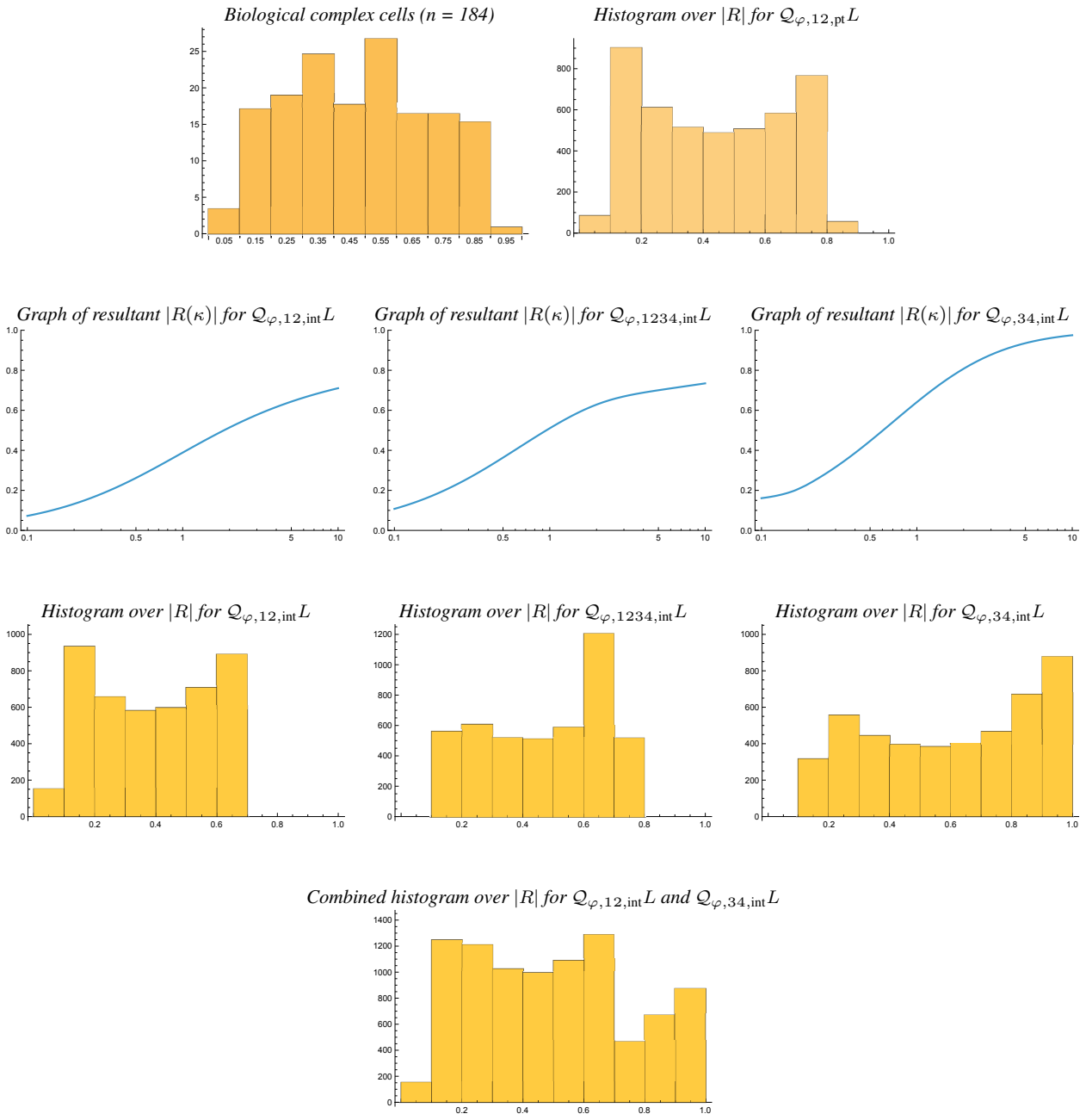

Fig. 4 Orientation selectivity analysis for the resultant of the orientation selectivity curves, with comparison to biological orientation selectivity histograms by Goris *et al.* (2015). **(first row, left)** Resultant histogram obtained from neurophysiological recordings of 184 complex cells in Macaque monkeys. **(first row, right)** Resultant histogram of the pointwise quasi quadrature measure $\mathcal{Q}_{\varphi,12,\mathrm{pt}}L$ according to (3) based on the previous analysis in (Lindeberg 2024a). **(second row)** Graphs of the resultant $|R|$ as function of the scale parameter ratio $\kappa = \sigma_2/\sigma_1$ for the integrated affine quasi quadrature measures $\mathcal{Q}_{\varphi,12,\mathrm{int}}L$, $\mathcal{Q}_{\varphi,1234,\mathrm{int}}L$ and $\mathcal{Q}_{\varphi,34,\mathrm{int}}L$ according to (11), (12) and (13). **(third row)** Histograms over the resultant $|R|$ for the integrated affine quasi quadrature measures $\mathcal{Q}_{\varphi,12,\mathrm{int}}L$, $\mathcal{Q}_{\varphi,1234,\mathrm{int}}L$ and $\mathcal{Q}_{\varphi,34,\mathrm{int}}L$ according to (11), (12) and (13), when assuming a uniform distribution over a logarithmic parameterization of the scale parameter ratio κ. **(fourth row)** Combined histogram of $\mathcal{Q}_{\varphi,12,\mathrm{int}}L$ and $\mathcal{Q}_{\varphi,34,\mathrm{int}}L$, when assuming equal numbers of complex cells for these two types. (Horizontal axes in rows 1, 3 and 4: 10 quantized bins over the resultant $|R| \in [0, 1]$. Vertical axes in rows 1, 3 and 4: bin counts.) (Horizontal axes in row 2: scale parameter ratio κ. Vertical axes in row 2: resultant $|R|$.)

to previous use of first- and second-order models of simple cells, and also to integrate non-linear transformations of such receptive field responses over extended regions in image space, when modelling the functional properties of complex cells.

4 Summary of discussion

We have presented a set of three new integrated affine quasi quadrature measures to model the functional properties of complex cells, and analyzed their orientation selectivity properties, based on the assumption that the receptive field shapes span a variability over the degree of elongation of the simple cells that form the input to these models of complex cells.

This analysis has been performed in three ways; in terms of: (i) orientation selectivity curves, (ii) graphs of the resultant $|R|$ as function of the scale parameter ratio $\kappa = \sigma_2/\sigma_1$ between the scale parameter σ_2 in the direction perpendicular to the preferred orientation of the receptive field and the scale parameter σ_1 in the direction of the preferred orientation of the receptive field, and (iii) histograms of the resultant $|R|$ when assuming a logarithmic distribution over the scale parameter ratio κ.

Specifically, by qualitative comparisons with the biological results by Nauhaus *et al.* (2008), regarding a significant variability in orientation selectivity properties of biological neurons from wide to narrow orientation selectivity properties, and to Goris *et al.* (2015), regarding orientation selectivity histograms over the resultant $|R|$, we have found that these results are consistent with a previously proposed hypothesis in Lindeberg (2023) further investigated in Lindeberg (2024a) that the receptive fields in the primary visual cortex should span a significant variability in the degree of elongation of the receptive fields. In this respect, the results are consistent with what becomes a natural consequence of stating desirable properties of an idealized vision system, that the receptive fields should be covariant under the natural geometric image transformations. In such a context, covariance properties of the family of receptive fields enable more accurate estimates of cues to the 3-D structure of the world, as the image data used as input to the vision system undergo significant variabilities, as caused by variations of the viewing conditions, such as the distance and the viewing direction between objects in the world and the observer.

Specifically, by simulating the orientation selectivity histograms that result from the presented new integrated affine quasi quadrature measures $\mathcal{Q}_{\varphi,12,\text{int}}L$, $\mathcal{Q}_{\varphi,1234,\text{int}}L$ and $\mathcal{Q}_{\varphi,34,\text{int}}L$ according to (11), (12) and (13), when combined with an assumption of a uniform distribution over the logarithm of the scale parameter ratio $\kappa = \sigma_2/\sigma_1$ of the receptive fields, we have found that the extensions of the previous pointwise quasi quadrature measure $\mathcal{Q}_{\varphi,12,\text{int}}L$ according to (3) offer ways of changing the shapes of the predicted orientation selectivity histograms regarding both how uniform the predicted histograms will be in relation to the previously recorded biological orientation selectivity histograms by Goris *et al.* (2015) and regarding the span of values of the resultant $|R|$ they cover.

Thus, we propose to: (i) include the mechanisms of spatial integration and including receptive field responses of higher order than 2 when modelling complex cells, and (ii) use similar criteria to match predicted orientation selectivity histograms to biological orientation selectivity histograms, as used in the presented analysis, to evaluate also other types of computational models for complex cells.

Let us finally remark that it should most likely be the case that the non-linear behaviour of complex cells may be more complex than the computational mechanisms used in the proposed idealized models in terms of integrated affine quasi quadrature measures. The overall purpose with this work is on the other hand to demonstrate that the orientation selectivity properties of the proposed idealized models of complex cells can be analyzed with a structurally similar methodology as used for probing the orientation selectivity properties of biological receptive fields. From this viewpoint, the comparison to the biological orientation selectivity histogram accumulated by Goris *et al.* (2015) is specifically to show that the gross behaviour in terms of an underlying distribution of receptive field shapes of different elongation can be used to reflect gross properties of the biological measurements. Our intention in this respect is to stimulate further tests of more complex computational models of complex cells, based on assuming distributions of the underlying receptive field shapes over the degree of elongation.

From the viewpoint of quasi quadrature models to be used for addressing computational tasks in computer vision, it should on the other hand also be mentioned that a hierarchical network constructed by applying a substantially simplified quasi quadrature model of complex cells in cascade can lead to quite reasonable results on computer vision benchmarks (Lindeberg 2020); see also the closely related work by Riesenhuber and Poggio (1999), Serre *et al.* (2007) and Pant *et al.* (2024).

References

L. Abballe and H. Asari. Natural image statistics for mouse vision. *PLoS ONE*, 17(1):e0262763, 2022.

E. Adelson and J. Bergen. Spatiotemporal energy models for the perception of motion. *Journal of Optical Society of America*, A 2: 284–299, 1985.

T. D. Albright. Direction and orientation selectivity of neurons in visual area MT of the macaque. *Journal of Neurophysiology*, 52(6): 1106–1130, 1984.

A. Almasi, H. Meffin, S. L. Cloherty, Y. Wong, M. Yunzab, and M. R. Ibbotson. Mechanisms of feature selectivity and invariance in primary visual cortex. *Cerebral Cortex*, 30(9):5067–5087, 2020.

P. Berkes and L. Wiskott. Slow feature analysis yields a rich repertoire of complex cell properties. *Journal of Vision*, 5(6):579–602, 2005.

R. N. Bracewell. *The Fourier Transform and its Applications*. McGraw-Hill, New York, 1999. 3rd edition.

M. Carandini. What simple and complex cells compute. *The Journal of Physiology*, 577(2):463–466, 2006.

M. Carandini and D. L. Ringach. Predictions of a recurrent model of orientation selectivity. *Vision Research*, 37(21):3061–3071, 1997.

S. G. Cogno and G. Mato. The effect of synaptic plasticity on orientation selectivity in a balanced model of primary visual cortex. *Frontiers in Neural Circuits*, 9:42, 2015.

B. R. Conway and M. S. Livingstone. Spatial and temporal properties of cone signals in alert macaque primary visual cortex. *Journal of Neuroscience*, 26(42):10826–10846, 2006.

A. De and G. D. Horwitz. Spatial receptive field structure of double-opponent cells in macaque V1. *Journal of Neurophysiology*, 125(3): 843–857, 2021.

G. C. DeAngelis and A. Anzai. A modern view of the classical receptive field: Linear and non-linear spatio-temporal processing by V1 neurons. In L. M. Chalupa and J. S. Werner, editors, *The Visual Neurosciences*, volume 1, pages 704–719. MIT Press, 2004.

G. C. DeAngelis, I. Ohzawa, and R. D. Freeman. Receptive field dynamics in the central visual pathways. *Trends in Neuroscience*, 18 (10):451–457, 1995.

W. Einhäuser, C. Kayser, P. König, and K. P. Körding. Learning the invariance properties of complex cells from their responses to natural stimuli. *European Journal of Neuroscience*, 15(3):475–486, 2002.

R. C. Emerson, M. C. Citron, W. J. Vaughn, and S. A. Klein. Nonlinear directionally selective subunits in complex cells of cat striate cortex. *Journal of Neurophysiology*, 58(1):33–65, 1987.

D. Ferster and K. D. Miller. Neural mechanisms of orientation selectivity in the visual cortex. *Annual Review of Neuroscience*, 23(1): 441–471, 2000.

A. Franciosini, V. Boutin, and L. Perrinet. Modelling complex cells of early visual cortex using predictive coding. In *Proc. 28th Annual Computational Neuroscience Meeting*, 2019. Available from https://laurentperrinet.github.io/publication/franciosini-perrinet-19-cns/franciosini-perrinet-19-cns.pdf.

M. A. Georgeson, K. A. May, T. C. A. Freeman, and G. S. Hesse. From filters to features: Scale-space analysis of edge and blur coding in human vision. *Journal of Vision*, 7(13):7.1–21, 2007.

M. Ghodrati, S.-M. Khaligh-Razavi, and S. R. Lehky. Towards building a more complex view of the lateral geniculate nucleus: Recent advances in understanding its role. *Progress in Neurobiology*, 156: 214–255, 2017.

R. L. T. Goris, E. P. Simoncelli, and J. A. Movshon. Origin and function of tuning diversity in Macaque visual cortex. *Neuron*, 88(4): 819–831, 2015.

M. Hansard and R. Horaud. A differential model of the complex cell. *Neural Computation*, 23(9):2324–2357, 2011.

D. Hansel and C. van Vreeswijk. The mechanism of orientation selectivity in primary visual cortex without a functional map. *Journal of Neuroscience*, 32(12):4049–4064, 2012.

T. Hansen and H. Neumann. A recurrent model of contour integration in primary visual cortex. *Journal of Vision*, 8(8):8.1–25, 2008.

D. J. Heeger. Normalization of cell responses in cat striate cortex. *Visual Neuroscience*, 9:181–197, 1992.

G. S. Hesse and M. A. Georgeson. Edges and bars: where do people see features in 1-D images? *Vision Research*, 45(4):507–525, 2005.

D. H. Hubel and T. N. Wiesel. Receptive fields of single neurones in the cat's striate cortex. *J Physiol*, 147:226–238, 1959.

D. H. Hubel and T. N. Wiesel. Receptive fields, binocular interaction and functional architecture in the cat's visual cortex. *J Physiol*, 160: 106–154, 1962.

D. H. Hubel and T. N. Wiesel. Receptive fields and functional architecture of monkey striate cortex. *The Journal of Physiology*, 195(1): 215–243, 1968.

D. H. Hubel and T. N. Wiesel. *Brain and Visual Perception: The Story of a 25-Year Collaboration*. Oxford University Press, 2005.

E. T. Jaynes. Prior probabilities. *Trans. on Systems Science and Cybernetics*, 4(3):227–241, 1968.

E. N. Johnson, M. J. Hawken, and R. Shapley. The orientation selectivity of color-responsive neurons in Macaque V1. *The Journal of Neuroscience*, 28(32):8096–8106, 2008.

J. Jones and L. Palmer. The two-dimensional spatial structure of simple receptive fields in cat striate cortex. *J. of Neurophysiology*, 58:1187–1211, 1987a.

J. Jones and L. Palmer. An evaluation of the two-dimensional Gabor filter model of simple receptive fields in cat striate cortex. *J. of Neurophysiology*, 58:1233–1258, 1987b.

J. J. Koenderink. The structure of images. *Biological Cybernetics*, 50 (5):363–370, 1984.

J. J. Koenderink and A. J. van Doorn. Representation of local geometry in the visual system. *Biological Cybernetics*, 55(6):367–375, 1987.

J. J. Koenderink and A. J. van Doorn. Generic neighborhood operators. *IEEE Transactions on Pattern Analysis and Machine Intelligence*, 14(6):597–605, Jun. 1992.

K. P. Kording, C. Kayser, W. Einhäuser, and P. Konig. How are complex cell properties adapted to the statistics of natural stimuli? *Journal of Neurophysiology*, 91(1):206–212, 2004.

D. G. Kristensen and K. Sandberg. Population receptive fields of human primary visual cortex organised as dc-balanced bandpass filters. *Scientific Reports*, 11(1):22423, 2021.

I. Lampl, J. S. Anderson, D. C. Gillespie, and D. Ferster. Prediction of orientation selectivity from receptive field architecture in simple cells of cat visual cortex. *Neuron*, 30(1):263–274, 2001.

Y.-T. Li, B.-H. Liu, X.-L. Chou, L. I. Zhang, and H. W. Tao. Synaptic basis for differential orientation selectivity between complex and simple cells in mouse visual cortex. *Journal of Neuroscience*, 35 (31):11081–11093, 2015.

Y. Lian, A. Almasi, D. B. Grayden, T. Kameneva, A. N. Burkitt, and H. Meffin. Learning receptive field properties of complex cells in V1. *PLoS Computational Biology*, 17(3):e1007957, 2021.

T. Lindeberg. A computational theory of visual receptive fields. *Biological Cybernetics*, 107(6):589–635, 2013.

T. Lindeberg. Dense scale selection over space, time and space-time. *SIAM Journal on Imaging Sciences*, 11(1):407–441, 2018.

T. Lindeberg. Provably scale-covariant continuous hierarchical networks based on scale-normalized differential expressions coupled in cascade. *Journal of Mathematical Imaging and Vision*, 62(1): 120–148, 2020.

T. Lindeberg. Normative theory of visual receptive fields. *Heliyon*, 7 (1):e05897:1–20, 2021. doi: 10.1016/j.heliyon.2021.e05897.

T. Lindeberg. Covariance properties under natural image transformations for the generalized Gaussian derivative model for visual receptive fields. *Frontiers in Computational Neuroscience*, 17: 1189949:1–23, 2023.

T. Lindeberg. Do the receptive fields in the primary visual cortex span a variability over the degree of elongation of the receptive fields? *arXiv preprint arXiv:2404.04858*, 2024a.

T. Lindeberg. Relationships between the degrees of freedom in the affine Gaussian derivative model for visual receptive fields and 2-D affine image transformations, with application to covariance properties of simple cells in the primary visual cortex. *arXiv preprint arXiv:2411.05673*, 2024b.

T. Lindeberg. Unified theory for joint covariance properties under geometric image transformations for spatio-temporal receptive fields according to the generalized Gaussian derivative model for visual receptive fields. *arXiv preprint arXiv:2311.10543*, 2024c.

T. Lindeberg. Orientation selectivity properties for the affine Gaussian derivative and the affine Gabor models for visual receptive fields. *Journal of Computational Neuroscience*, 53(1):61–98, 2025.

T. Lindeberg and J. Gårding. Shape-adapted smoothing in estimation of 3-D shape cues from affine distortions of local 2-D structure. *Image and Vision Computing*, 15(6):415–434, 1997.

D. G. Lowe. Towards a computational model for object recognition in IT cortex. In *Biologically Motivated Computer Vision*, volume 1811 of *Springer LNCS*, pages 20–31. Springer, 2000.

S. Marcelja. Mathematical description of the responses of simple cortical cells. *Journal of Optical Society of America*, 70(11):1297–1300, 1980.

L. M. Martinez and J.-M. Alonso. Construction of complex receptive fields in cat primary visual cortex. *Neuron*, 32(3):515–525, 2001.

K. A. May and M. A. Georgeson. Blurred edges look faint, and faint edges look sharp: The effect of a gradient threshold in a multi-scale edge coding model. *Vision Research*, 47(13):1705–1720, 2007.

B. Merkt, F. Schüßler, and S. Rotter. Propagation of orientation selectivity in a spiking network model of layered primary visual cortex. *PLoS Computational Biology*, 15(7):e1007080, 2019.

P. Merolla and K. Boahn. A recurrent model of orientation maps with simple and complex cells. In *Advances in Neural Information Processing Systems (NIPS 2004)*, pages 995–1002, 2004.

S. Moldakarimov, M. Bazhenov, and T. J. Sejnowski. Top-down inputs enhance orientation selectivity in neurons of the primary visual cortex during perceptual learning. *PLoS Computational Biology*, 10 (8):e1003770, 2014.

J. A. Movshon, E. D. Thompson, and D. J. Tolhurst. Receptive field organization of complex cells in the cat's striate cortex. *The Journal of Physiology*, 283(1):79–99, 1978.

I. Nauhaus, A. Benucci, M. Carandini, and D. L. Ringach. Neuronal selectivity and local map structure in visual cortex. *Neuron*, 57(5): 673–679, 2008.

G. Nguyen and A. W. Freeman. A model for the origin and development of visual orientation selectivity. *PLoS Computational Biology*, 15(7):e1007254, 2019.

P. Nguyen, J. Sooriyaarachchi, Q. Huang, and C. L. J. Baker. Estimating receptive fields of simple and complex cells in early visual cortex: A convolutional neural network model with parameterized rectification. *PLOS Computational Biology*, 20(5):e1012127, 2024.

T. D. Oleskiw, J. D. Lieber, E. P. Simoncelli, and J. A. Movshon. Foundations of visual form selectivity for neurons in macaque V1 and V2. *bioRxiv*, 2024.03.04.583307, 2024.

N. Pant, I. F. Rodriguez, A. Beniwal, S. Warren, and T. Serre. HMAX strikes back: Self-supervised learning of human-like scale invariant representations. In *Cognitive Computational Neuroscience*, 2024. https://2024.ccneuro.org/pdf/533_Paper_authored_CCN_2024_HMAX-(2).pdf.

J. J. Pattadkal, G. Mato, C. van Vreeswijk, N. J. Priebe, and D. Hansel. Emergent orientation selectivity from random networks in mouse visual cortex. *Cell Reports*, 24(8):2042–2050, 2018.

Z.-J. Pei, G.-X. Gao, B. Hao, Q.-L. Qiao, and H.-J. Ai. A cascade model of information processing and encoding for retinal prosthesis. *Neural Regeneration Research*, 11(4):646, 2016.

M. Porat and Y. Y. Zeevi. The generalized Gabor scheme of image representation in biological and machine vision. *IEEE Transactions on Pattern Analysis and Machine Intelligence*, 10(4):452–468, 1988.

N. J. Priebe. Mechanisms of orientation selectivity in the primary visual cortex. *Annual Review of Vision Science*, 2:85–107, 2016.

M. Riesenhuber and T. Poggio. Hierarchical models of object recognition in cortex. *Nature*, 2(11):1019–1025, 1999.

D. L. Ringach. Spatial structure and symmetry of simple-cell receptive fields in macaque primary visual cortex. *Journal of Neurophysiology*, 88:455–463, 2002.

D. L. Ringach. Mapping receptive fields in primary visual cortex. *Journal of Physiology*, 558(3):717–728, 2004.

D. L. Ringach, R. M. Shapley, and M. J. Hawken. Orientation selectivity in macaque V1: Diversity and laminar dependence. *Journal of Neuroscience*, 22(13):5639–5651, 2002.

D. Rose and C. Blakemore. An analysis of orientation selectivity in the cat's visual cortex. *Experimental Brain Research*, 20:1–17, 1974.

M. A. Ruslim, A. N. Burkitt, and Y. Lian. Learning spatio-temporal V1 cells from diverse LGN inputs. *bioRxiv*, pages 2023–11, 2023.

N. C. Rust, O. Schwartz, J. A. Movshon, and E. P. Simoncelli. Spatiotemporal elements of macaque V1 receptive fields. *Neuron*, 46 (6):945–956, 2005.

S. Sadeh and S. Rotter. Statistics and geometry of orientation selectivity in primary visual cortex. *Biological Cybernetics*, 108:631–653, 2014.

K. S. Sasaki, R. Kimura, T. Ninomiya, Y. Tabuchi, H. Tanaka, M. Fukui, Y. C. Asada, T. Arai, M. Inagaki, T. Nakazono, M. Baba, K. Daisuke, S. Nishimoto, T. M. Sanada, T. Tani, K. Imamura, S. Tanaka, and I. Ohzawa. Supranormal orientation selectivity of visual neurons in orientation-restricted animals. *Scientific Reports*, 5(1):16712, 2015.

P. H. Schiller, B. L. Finlay, and S. F. Volman. Quantitative studies of single-cell properties in monkey striate cortex. II. Orientation specificity and ocular dominance. *Journal of Neurophysiology*, 39(6): 1320–1333, 1976.

B. Scholl, A. Y. Y. Tan, J. Corey, and N. J. Priebe. Emergence of orientation selectivity in the mammalian visual pathway. *Journal of Neuroscience*, 33(26):10616–10624, 2013.

P. Seriès, P. E. Latham, and A. Pouget. Tuning curve sharpening for orientation selectivity: coding efficiency and the impact of correlations. *Nature Neuroscience*, 7(10):1129–1135, 2004.

T. Serre and M. Riesenhuber. Realistic modeling of simple and complex cell tuning in the HMAX model, and implications for invariant object recognition in cortex. Technical Report AI Memo 2004-017, MIT Computer Science and Artifical Intelligence Laboratory, 2004.

T. Serre, L. Wolf, S. Bileschi, M. Riesenhuber, and T. Poggio. Robust object recognition with cortex-like mechanisms. *IEEE Transactions on Pattern Analysis and Machine Intelligence*, 29(3):411–426, 2007.

R. Shapley, M. Hawken, and D. L. Ringach. Dynamics of orientation selectivity in the primary visual cortex and the importance of cortical inhibition. *Neuron*, 38(5):689–699, 2003.

D. C. Somers, S. B. Nelson, and M. Sur. An emergent model of orientation selectivity in cat visual cortical simple cells. *Journal of Neuroscience*, 15(8):5448–5465, 1995.

H. Sompolinsky and R. Shapley. New perspectives on the mechanisms for orientation selectivity. *Current Opinion in Neurobiology*, 7(4): 514–522, 1997.

J. Touryan, B. Lau, and Y. Dan. Isolation of relevant visual features from random stimuli for cortical complex cells. *Journal of Neuroscience*, 22(24):10811–10818, 2002.

J. Touryan, G. Felsen, and Y. Dan. Spatial structure of complex cell receptive fields measured with natural images. *Neuron*, 45(5):781–791, 2005.

R. L. D. Valois, N. P. Cottaris, L. E. Mahon, S. D. Elfer, and J. A. Wilson. Spatial and temporal receptive fields of geniculate and cortical cells and directional selectivity. *Vision Research*, 40(2):3685–3702, 2000.

J. P. van Kleef, , S. L. Cloherty, and M. R. Ibbotson. Complex cell receptive fields: evidence for a hierarchical mechanism. *The Journal of Physiology*, 588(18):3457–3470, 2010.

E. Y. Walker, F. H. Sinz, E. Cobos, T. Muhammad, E. Froudarakis, P. G. Fahey, A. S. Ecker, J. Reimer, X. Pitkow, and A. S. Tolias. Inception loops discover what excites neurons most using deep predictive models. *Nature Neuroscience*, 22(12):2060–2065, 2019.

S. A. Wallis and M. A. Georgeson. Mach edges: Local features predicted by 3rd derivative spatial filtering. *Vision Research*, 49(14): 1886–1893, 2009.

H. Wang, O. Dey, W. N. Lagos, N. Behnam, E. M. Callaway, and B. K. Stafford. Parallel pathways carrying direction-and orientation-selective retinal signals to layer 4 of the mouse visual cortex. *Cell*

Reports, 43(3), 2024.

Q. Wang and M. W. Spratling. Contour detection in colour images using a neurophysiologically inspired model. *Cognitive Computation*, 8(6):1027–1035, 2016.

D. W. Watkins and M. A. Berkley. The orientation selectivity of single neurons in cat striate cortex. *Experimental Brain Research*, 19:433–446, 1974.

W. Wei, B. Merkt, and S. Rotter. A theory of orientation selectivity emerging from randomly sampling the visual field. *bioRxiv*, pages 2022–07, 2022.

G. Wendt and F. Faul. Binocular luster elicited by isoluminant chromatic stimuli relies on mechanisms similar to those in the achromatic case. *Journal of Vision*, 24(3):7–7, 2024.

H. Yedjour and D. Yedjour. A spatiotemporal energy model based on spiking neurons for human motion perception. *Cognitive Neurodynamics*, pages 1–15, 2024.

R. A. Young. The Gaussian derivative model for spatial vision: I. Retinal mechanisms. *Spatial Vision*, 2(4):273–293, 1987.

R. A. Young and R. M. Lesperance. The Gaussian derivative model for spatio-temporal vision: II. Cortical data. *Spatial Vision*, 14(3, 4): 321–389, 2001.

R. A. Young, R. M. Lesperance, and W. W. Meyer. The Gaussian derivative model for spatio-temporal vision: I. Cortical model. *Spatial Vision*, 14(3, 4):261–319, 2001.